ELSEVIER

Toxicon 47 (2006) 75–86

TOXICON

www.elsevier.com/locate/toxicon

Calcium plays a key role in the effects induced by a snake venom Lys49 phospholipase A_2 homologue on a lymphoblastoid cell line

Rodrigo Mora [a,b], Alexis Maldonado [c], Berta Valverde [d], José María Gutiérrez [b,*]

[a] *Departamento de Microbiología e Inmunología, Facultad de Microbiología, Universidad de Costa Rica, San José, Costa Rica*
[b] *Instituto Clodomiro Picado, Facultad de Microbiología, Universidad de Costa Rica, San José, Costa Rica*
[c] *Escuela de Ingeniería Eléctrica, Facultad de Ingeniería, Universidad de Costa Rica*
[d] *Laboratorio de Estudios Especializados, Hospital Nacional de Niños Dr Carlos Sáenz Herrera, Caja Costarricense del Seguro Social, San José, Costa Rica*

Received 9 August 2005; revised 7 October 2005; accepted 8 October 2005
Available online 21 November 2005

Abstract

A catalytically-inactive Lys49 phospholipase A_2 homologue from the venom of the snake *Bothrops asper* induces diverse effects (necrosis, apoptosis and proliferation) in a lymphoblastoid cell line, depending on the toxin concentration. The increments in cytosolic Ca^{2+} levels induced by this toxin in this cell line were assessed. At high toxin concentration (100 μg/mL) the toxin induces drastic disruption of the plasma membrane, associated with a prominent Ca^{2+} influx and necrosis. Previous incubation of the cells with the chelating agent EGTA or with ruthenium red, an inhibitor of the uniporter mitochondrial Ca^{2+} transport, greatly reduced necrosis. At a toxin concentration of 12.5 μg/mL, apoptosis is the predominant response, being associated with lower increments in cytosolic Ca^{2+}. This effect was inhibited by preincubation with ruthenium red and the cytosolic Ca^{2+} chelator BAPTA-AM. The proliferative response, which occurs at a low toxin concentration (0.5 μg/mL), is associated with a small and oscillatory increment in cytosolic Ca^{2+}. It was inhibited by EGTA, ruthenium red and BAPTA-AM, by inhibitors of the endoplasmic reticulum Ca^{2+}-ATPase (SERCA) and by blockade of the ryanodine receptor. It is concluded that necrosis and apoptosis induced by this toxin are associated with increments in cytosolic Ca^{2+} levels following plasma membrane perturbation, together with the involvement of mitochondria. The cellular proliferative response depends on a limited Ca^{2+} influx through the plasma membrane, being associated with a concerted functional unit constituted by SERCA, the ryanodine receptor and mitochondria, which regulate the observed oscillations in cytosolic Ca^{2+} concentration.

Keywords: Ca2+ homeostasis; Snake venom; Lys49 phospholipase A2; Mitochondria; SERCA; Plasma membrane; Necrosis; Apoptosis

1. Introduction

Phospholipases A_2 (PLA_2s) catalyze the Ca^{2+}-dependent hydrolysis of the fatty acyl ester bond at the sn-2 position of glycerophospholipids, and are grouped into different classes depending on disulfide bridge positions and lengths of C-termini (Dennis, 1994). Snake venoms constitute an extremely rich source of PLA_2s (Rosenberg, 1990), belonging to PLA_2 classes I (elapid PLA_2s) and II (viperid PLA_2s) (Six and Dennis, 2000; Valentin and Lambeau, 2000). These venom enzymes have evolved through an accelerated process of mutation in the coding regions of their genes (Kini and Chan, 1999; Ohno et al., 2002, 2003), which has contributed to the generation of a highly complex toxicological and pharmacological profile

* Corresponding author. Tel.: +506 2293135; fax: +506 2920485.
E-mail address: jgutierr@icp.ucr.ac.cr (J.M. Gutiérrez).

0041-0101/$ - see front matter © 2006 Elsevier Ltd. All rights reserved.
doi:10.1016/j.toxicon.2005.10.001

associated with the acquisition of neurotoxic, myotoxic, cytotoxic, anticoagulant, hemolytic, hypotensive, platelet-aggregation inhibiting, and proinflammatory effects (Kini, 1997).

Viperid snake venoms, such as those of the species of the genus *Bothrops*, induce prominent local tissue damage in the victims, associated with myonecrosis, hemorrhage, blistering and edema (Gutiérrez and Lomonte, 1989, 2003). Skeletal muscle necrosis, myonecrosis, is predominantly caused by a group of basic PLA_2s which directly affect the integrity of muscle cell plasma membrane, promoting a rapid degenerative process that ends in irreversible cell damage (Gutiérrez and Ownby, 2003). In addition to myotoxicity, these basic PLA_2s are able to affect other mammalian cell types in culture (Bultrón et al., 1993; Brusés et al., 1993; Lomonte et al., 1994a), being also bactericidal (Páramo et al., 1998). Moreover, they also induce pain (Chacur et al., 2003) and edema (Teixeira et al., 2003). *Bothrops* sp myotoxic PLA_2s include catalytically-active variants, named Asp49 PLA_2s, as well as catalytically-inactive homologues, known as Lys49 PLA_2s, which present various substitutions in the Ca^{2+}-binding loop and at position 49, where Lys replaces the highly conserved Asp (Ownby et al., 1999; Lomonte et al., 2003). Such modifications drastically affect the ability of these proteins to bind calcium, required for catalysis, rendering these homologues enzymatically inactive (van den Bergh et al., 1988; Ward et al., 2002). Interestingly, these Lys49 PLA_2 homologues are highly cytotoxic, myotoxic, bactericidal and proinflammatory (Lomonte et al., 2003), evidencing that phospholipid hydrolysis is not strictly required for these activities.

A Lys49 PLA_2 homologue from the venom of *Bothrops asper* was recently shown to induce a complex pattern of effects on a lymphoblastoid cell line, depending on the toxin concentration used (Mora et al., 2005). Overt cytotoxicity, i.e. necrosis, was observed at high concentrations, whereas lower levels induced apoptosis, and still lower concentrations promoted a proliferative response (Mora et al., 2005). However, the cellular mechanisms involved in these highly disparate outcomes are unknown at present. Ca^{2+} may be a common mediator of these effects since it plays a key role in many cellular processes, both physiological (Berridge et al., 2003) and pathological (Orrenius et al., 2003). The specificity of Ca^{2+}-mediated responses is strictly dependent on its spatial-temporal behavior associated with a complex interplay of components of the so called 'Ca^{2+} toolkit' (Berridge et al., 2003; Goldbeter, 2002).

It has been proposed that the drastic pathological alterations induced by venom myotoxic PLA_2s on muscle cells are initiated by an early plasma membrane disruption which promotes a rapid Ca^{2+} influx, thereby starting a series of intracellular degenerative processes (Gutiérrez et al., 1984; Harris and Cullen, 1990; Gutiérrez and Ownby, 2003). However, the role of such Ca^{2+} influx in PLA_2-induced cellular toxicity has not been conclusively demonstrated, nor has been the participation of this cation in other, non-necrotic outcomes, such as apoptosis and proliferation, induced by myotoxic PLA_2s. The aim of this study was to determine the participation of Ca^{2+} in necrosis, apoptosis and proliferation induced by a Lys49 PLA_2 in a lymphoblastoid cell line, which has been previously used as a cellular model to investigate the effects of this myotoxin.

2. Materials and methods

2.1. Lys49 PLA_2 homologue and cell line

Myotoxin II, a Lys49 PLA_2, was isolated from a pool of venom obtained from adult specimens of *Bothrops asper* collected in the Atlantic region of Costa Rica. Isolation was performed by two cycles of ion-exchange chromatography on CM-Sephadex C-25, as previously described (Lomonte and Gutiérrez, 1989). Homogeneity of the preparation was demonstrated by SDS-PAGE run under reducing conditions (Laemmli, 1970). The toxin was devoid of enzymatic PLA_2 activity even at doses as high as 100 μg protein, assessed by a titrimetric procedure previously described (Gutiérrez et al., 1986). The lymphoblastoid B cell line CRL-8062 (ATCC) was propagated in suspension using RPMI 1640 medium supplemented with 2 mM L-glutamine and 10% fetal bovine serum (FBS). These are diploid cells and were used within the first passages. Cultures were maintained at cell densities between 1×10^5 and 1×10^6 cells/mL, and medium was changed every 2–3 days. When performing the assays described below, the medium was supplemented with 1% FBS.

2.2. Inhibitors

The role of extracellular Ca^{2+} was assessed using 2 mM EGTA (Shakhman et al., 2003). Cytosolic Ca^{2+} was inhibited with 1,2-bis(aminophenoxy)-ethane-*N*,*N*,*N*'-tetra-acetic acid (BAPTA-AM, 50 μM) (Shakhman et al., 2003). The participation of mitochondria was evaluated by using ruthenium red (10 μM), an inhibitor of the mitochondrial Ca^{2+} uniporter (Shakhman et al., 2003; Vázquez-Martínez et al., 2003). The intracellular Ca^{2+} stores were evaluated by using the inhibitors of sarcoplasmic reticulum Ca^{2+}-ATPase (SERCA) thapsigargin (10 μM) (Rigual et al., 2002; Cudd et al., 2003) and cyclopiazonic acid (10 μM) (Rigual et al., 2002). When studying the proliferative effect, the role of ryanodine-sensitive channels was assessed using ryanodine, which is inhibitory at 10 μM, and stimulatory at lower concentrations (10–100 nM) (Johnson et al., 2002). In addition, inhibition of the Ca^{2+} -sensitive ryanodine channels was performed by using $MgCl_2$ (Cudd et al., 2003; Vázquez-Martínez et al., 2003). All the experiments involving inhibition of Ca^{2+}-regulation pathways were carried out by incubating cells with the inhibitors at 37 °C

during one hour before the addition of the myotoxin. In some experiments, the effects of the Ca^{2+} ionophore A23187 were investigated by incubating it, at various concentrations, with cell cultures for 24 and 48 h. All the inhibitors used and the ionophore A23187 were purchased from Sigma-Aldrich (St Louis, MO).

2.3. Quantification of cytosolic Ca^{2+} by flow cytometry

An assay based on the simultaneous use of the fluorochromes Fura-Red (Sigma-Aldrich) and Fluo-3 (Molecular Probes, Eugene, OR) was performed (Novak and Rabinovitch, 1994; Burchiel et al., 2000). Briefly, cells (4×10^6/mL) were incubated with 6 μM Fluo-3, 6 μM Fura-Red and 0.1% Pluronic detergent (Molecular Probes) for 60 min at 37 °C. Then, cells were washed with phosphate-buffered saline solution, pH 7.2 (PBS) and resuspended in RPMI, supplemented with 1% FBS, to obtain a suspension of 2×10^6 cells/mL. Cells were then incubated with various concentrations of MT-II during different time intervals and analyzed in a FACSCalibur flow cytometer (BD Immunocytochemistry Systems, San Jose, CA) with an argon laser excitation. The green fluorescence of Fluo-3 was quantified with filters set FL-1, and the red fluorescence of Fura-Red with FL-3 (Novak and Rabinovitch, 1994). Both measurements were performed for approximately 400 sec to obtain an average value for this incubation time. Viable, well stained cells were discriminated from dead cells, cellular detritus and unstained cells by the parameters of frontal light dispersion (FSC), at 90° angle (SSC) and fluorescence 3, according to Bunn et al. (1990). Data analysis was carried out with the program Cell Quest Pro^R.

In order to correlate increments in cytosolic Ca^{2+} with plasma membrane disruption, cells (2×10^6/mL) were incubated in RPMI medium with 6 μM Fluo-3 AM for 60 min, in a total volume of 400 μL, before the addition of MT-II. Then, cell suspensions were additionally incubated for 20 min. Immediately before determining changes in cytosolic Ca^{2+}, as described above, 20 μL of a solution of propidium iodide (PI, 50 μg/mL) were added; the green fluorescence of Fluo-3 and the red fluorescence of PI were measured in a FACSCalibur flow cytometer. Data were analyzed with the Cell Quest Pro^R Program.

2.4. Quantification of cytosolic Ca^{2+} in small groups of cells

In order to follow changes in cytosolic Ca^{2+} in individual cells and small groups of cells within the first seconds after MT-II addition, a fluorescence microscope system, which uses digital cameras connected to a computer for image analysis, was employed, using the fluorescent dye Indo-1. A working solution of Indo-1 AM (Molecular Probes) was prepared by diluting a stock solution (dissolved in DMSO) in PBS, in order to obtain final concentrations of 20 μM Indo-1 and 0.2% Pluronic detergent. One volume of this solution was mixed with one volume of the cell suspension, and the mixture was incubated for 1 h at 37 °C. Then, cells were washed once with PBS and, after 30 min, they were centrifuged and resuspended in RPMI supplemented with 1% FBS. In order to prevent oxidative degradation of Indo-1 by UV light, the antioxidant Trolox (OXIS, Portland, OR, 500 μM) was added (Scheenen et al., 1996). Addition of Trolox did not induce any discernible effect in the evaluated responses. Aliquots of cell suspensions were transferred to Neubauer chambers and the effect of MT-II was assessed in a fluorescence microscope. A prototype for the acquisition of fluorescent images, which uses two black and white analog cameras, was built. It includes a dichroic cube with an emission filter of 340 nm and two filters of 400 and 480 nm located at the ocular lenses of the microscope. The two CCD cameras were connected to a video capture card, and two images per second per camera were obtained. The images measured 640×480 pixels, with a pixel depth of 8 bits. A Computer Vision program in C++ was developed for the real-time data acquisition, using a Video4Linux interface and running on a Debian GNU/Linux system. The images from the two cameras were aligned to be able to analyze their intensity pixel per pixel, and a segmentation step was performed to automatically identify and separate the cells from the background. The effects of MT-II were assessed by performing consecutive determinations of changes in the ratio of the signal intensities from the cells on both cameras. This ratio (R) is directly related to cytosolic Ca^{2+} concentration by the following expression: $[Ca^{2+}] = Kd\,[(R-R_{min})/(R_{max}-R)]$ (F480max/F480 min), to achieve a ratiometric Ca^{2+} quantification (Williams and Fay, 1990). Controls included cells incubated with medium alone. The system was calibrated calculating the value of Kd every day an experiment was run, by an adaptation of the method of Williams and Fay (1990), using various ratios of 10 mM K_2EGTA and 10 mM CaEGTA, in 100 mM KCl, 30 mM MOPS, pH 7.2 buffer, and the ionophore A23187 (Ca^{2+} calibration kit, Molecular Probes).

2.5. Quantification of necrosis and cell proliferation

Cell proliferation and necrosis were determined using the chromophore XTT (Sigma-Aldrich), which allows the estimation of the number of viable cells spectrophotometrically as a function of their oxidative status (Su et al., 2003; Mora et al., 2005). Briefly, 100 μL of a cell suspension (2×10^6 cells/mL) were incubated with 100 μL of MT-II (0.5 μg/mL to study proliferation, and 100 μg/mL to study necrosis). Cells were preincubated with medium alone or with the different inhibitors of Ca^{2+} fluxes and transport systems at 37 °C for 1 h before the addition of MT-II. After 24 h of incubation of cells with MT-II, 50 μL of the labeling mixture (1 mg/mL XTT in PBS and 1 mM phenazine methosulfate) were added to each well and incubation was continued for 3 h in the dark. Absorbances were then

recorded in a microplate reader against a 650 nm reference filter. A blank well containing only PBS and the labeling mixture was included for background correction.

2.6. Quantification of apoptosis

A TUNEL assay was performed using the APO-DIRECT kit (Pharmingen, San Diego, CA), which uses deoxynucleotides directly conjugated to fluorochromes (Li et al., 1995; Mora et al., 2005). Cells that had been preincubated with the various inhibitors of Ca^{2+}, and then incubated with MT-II (12.5 μg/mL) for 48 h, were suspended in PBS, fixed in 1% paraformaldehyde in PBS, and placed on ice for 15 min. After a washing step with PBS, cells were resuspended in ice-cold 70% ethanol and kept in the freezer before staining. Cells were washed twice with the kit's washing solution and resuspended in 50 μL of staining solution (0.75 μL TdT enzyme, 8 μL FITC-dUTP, 10 μL reaction buffer and 32 μL of distilled water per sample). Cells were incubated overnight at room temperature and then washed twice with the kit's rinse buffer. Cellular pellets were then suspended in 0.5 mL of the PI/RNASE solution (5 μg/mL PI and 200 μg(mL RNAse), incubated for 30 min at room temperature, and analyzed by flow cytometry. Cells were excited with a blue Argon laser (15 mW) at 488 nm. The FITC-dUTP fluorescence was recorded in the FL-1 filter set (530/30 nm) and the red fluorescence

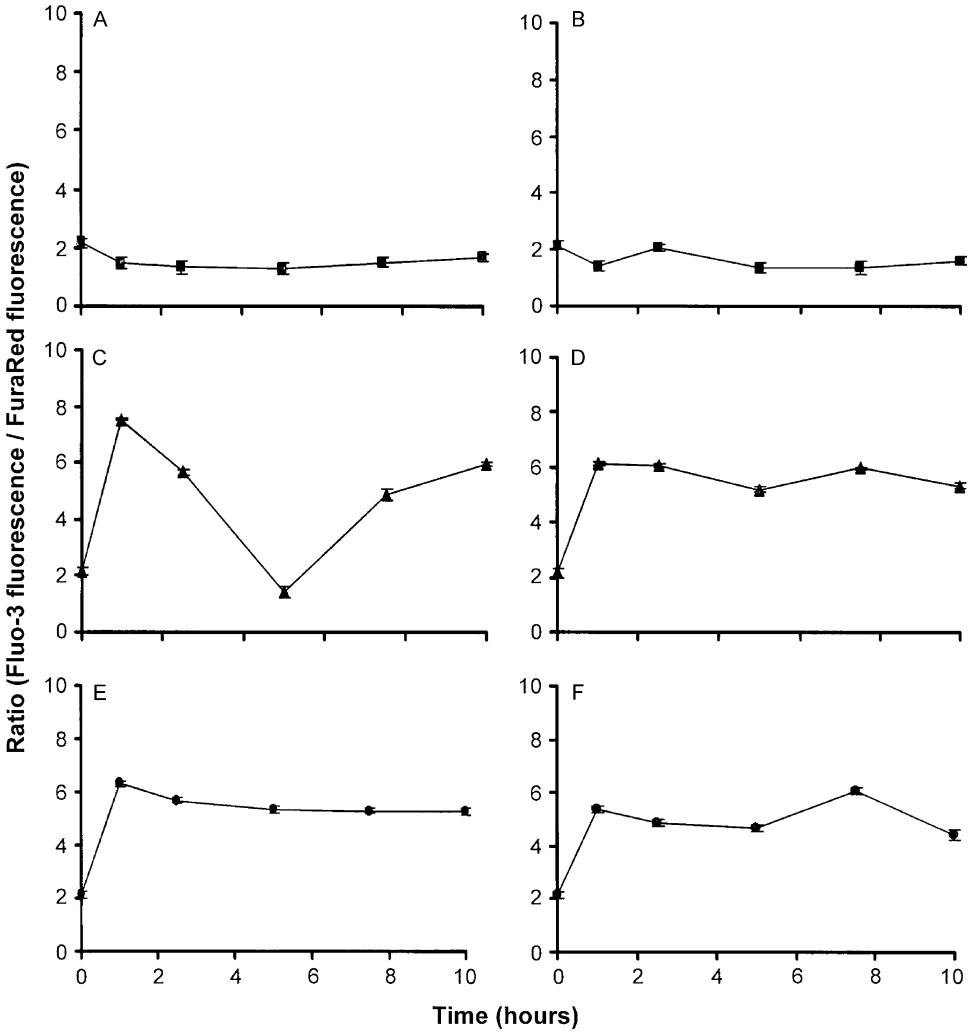

Fig. 1. Flow cytometric analysis of the changes in cytosolic Ca^{2+} concentration in lymphoblastoid cells incubated with various concentrations of MT-II. Increments in cytosolic Ca^{2+} levels were followed by the increase in the ratio of fluorescence of Fluo-3 and Fura-Red. (A) Cells incubated with medium with no toxin. (B) to (F) Cells incubated with the following concentrations of MT-II: (B) 0.5 μg/mL, (C) 12.5 μg/mL, (D) 25 μg/mL, (E) 50 μg/mL, and (F) 100 μg/mL. Each point corresponds to approximately 10,000 cells.

of PI was recorded in the FL-2 (585/30 nm) filter set. Data from 10^4 cells were collected and analyzed using the CellQuest software (Becton Dickinson).

2.7. Statistical analysis

The homogeneity of variance in each set of data was evaluated by the Box M method, and normality was assessed by the Shapiro-Wilk test. In both cases, differences were considered significant for P values <0.05. The Student's t test and the Mann–Whitney test were used to determine the significance of the differences between pairs of means. When more than two groups were compared, analysis of variance, followed by Tukey Honest test, was performed. All statistical analyses were carried out using the software package STATISTICA.

3. Results

3.1. Effects of MT-II on cytosolic Ca^{2+}

When cells were incubated with 0.5 μg/mL MT-II, a concentration that does not induce cytotoxicity but promotes a proliferative response (Mora et al., 2005), no changes were detected in cytosolic Ca^{2+} by flow cytometry (Fig. 1). However, when Ca^{2+} concentration was studied in individual groups of cells by fluorescence microscopy, an oscillatory increment which reached cytosolic concentrations of 4 μM was observed within the first seconds of addition of the toxin (Fig. 2C). A concentration of MT-II of 12.5 μg/mL, which causes apoptosis in this cell type (Mora et al., 2005), induced a transient increase in cytosolic Ca^{2+}, followed by a decrease, as detected by flow cytometry (Fig. 1). At this concentration, the microscopic system detected an increment in cytosolic Ca^{2+} up to a concentration of 10μM in individual groups of cells within the first 30 s of incubation (Fig. 2B). A sustained increment in cytosolic Ca^{2+} was observed in both flow cytometric and microscopic systems at MT-II concentrations $\geq$25 μg/mL (Figs. 1 and 2A), which are known to induce apoptosis and, predominantly, necrosis (Mora et al., 2005).

3.2. Relationship between plasma membrane disruption and increments in cytosolic Ca^{2+}

When cells loaded with Fluo-3 were incubated with various concentrations of MT-II, in the presence of PI, a simultaneous determination of cytosolic Ca^{2+} and plasma membrane disruption could be performed by flow cytometry, by following changes in Fluo-3 fluorescence and nucleic acid staining by PI, respectively. There was an increment in the number of cells showing simultaneous increments in cytosolic Ca^{2+} and staining by PI, when incubations with MT-II were performed for either 20 min (Fig. 3) or 24 h (not shown). In contrast, there was not an increment in the population of cells with increased cytosolic Ca^{2+} and with no PI labelling (Fig. 3); these findings suggest that the observed Ca^{2+} influx occurred mostly through damaged plasma membrane.

3.3. Role of Ca^{2+} in MT-II-induced necrosis

Previous work showed that MT-II, at a concentration of 100 μg/mL, induced a conspicuous cytotoxic effect with morphological features characteristic of necrotic cell death (Mora et al., 2005). When cells were preincubated with various compounds that affect Ca^{2+} homeostasis, before the addition of MT-II (100 μg/mL), a significant inhibition of cytotoxicity was achieved by the use of EGTA and ruthenium red (Fig. 4A). In contrast, preincubation with the cytosolic Ca^{2+} chelator BAPTA-AM did not affect the cytotoxic response (Fig. 4A). The drastic and rapid increment in cytosolic Ca^{2+} induced by this concentration of MT-II was significantly abrogated when cells were incubated with EGTA (Fig. 2A).

3.4. Role of Ca^{2+} in MT-II-induced apoptosis

A concentration of 12.5 μg/mL MT-II, which promoted increments in cytosolic Ca^{2+} (Figs. 1 and 2B), was used to induce apoptosis in lymphoblastoid cells upon a 48 h incubation (Mora et al., 2005). Preincubation of cells with EGTA for 48 h induced apoptosis, and therefore this chelating agent could not be tested for its inhibitory role. On the other hand, both BAPTA-AM and ruthenium red significantly reduced apoptosis induced by MT-II (Fig. 4B). As a control, incubation of cells with the ionophore A23187 (25 μM) for 24 h induced apoptosis (Fig. 4B).

3.5. Role of Ca^{2+} in MT-II-induced cellular proliferation

When lymphoblastoid cells were incubated with a low MT-II concentration (0.5 μg/mL), a proliferative response occurred, as previously described by XTT reduction assay and confirmed by cell cycle analysis through flow cytometry (Mora et al., 2005). At this toxin concentration, there was a relatively small and oscillatory increment in cytosolic Ca^{2+} (Fig. 2C). As a control, 5 μM A23187 also induced a proliferative response, whereas higher concentrations of this ionophore induced cytotoxicity (Fig. 5B). Preincubation of cells with EGTA, BAPTA-AM and ruthenium red, before the addition of MT-II, abrogated the proliferative effect (Fig. 5A). In order to investigate the role of intracellular Ca^{2+} reserves in this effect, pretreatment with the SERCA inhibitors thapsigargin and cyclopiazonic acid was performed. Both of these compounds inhibited the proliferative response (Fig. 6). Furthermore, ryanodine (10 μM) and $MgCl_2$, inhibitors of the ryanodine channel that participates in the Ca^{2+}-induced Ca^{2+} release (CICR), were shown to inhibit the proliferative response

as well (Fig. 6). In contrast, lower, stimulatory concentrations of ryanodine (10 and 100 nm) induced a proliferative effect in the absence of MT-II (Fig. 6), thus reproducing MT-II-induced effect.

4. Discussion

MT-II has been characterized as a myotoxic and cytotoxic Lys49 PLA_2 homologue which also promotes

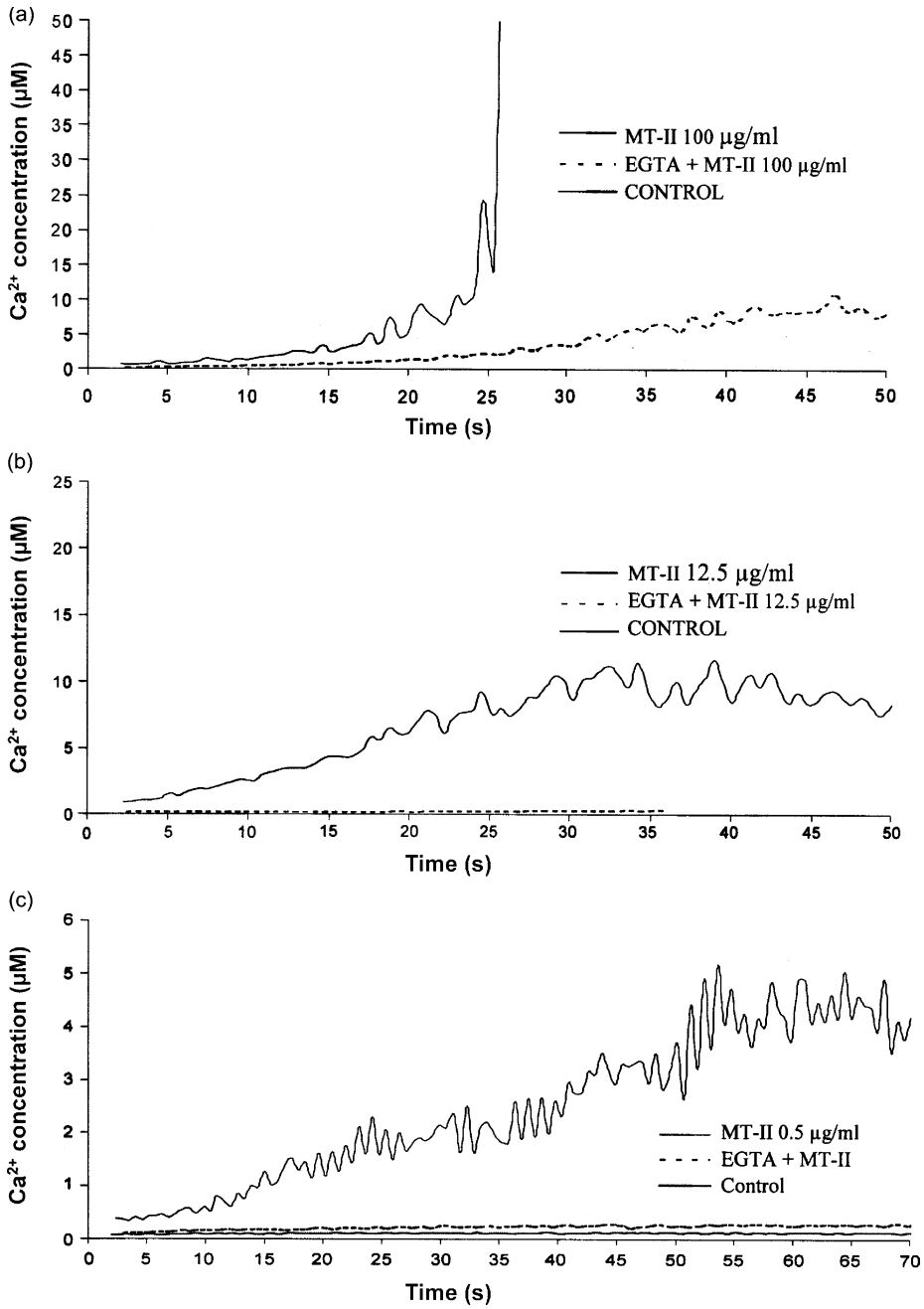

Fig. 2. Changes in cytosolic Ca^{2+} concentration determined by fluorescence microscopy, using Indo-1 AM as probe, in a group of lymphoblastoid cells during the first seconds after addition of 100 μg/mL (A), 12.5 μg/mL (B) and 0.5 μg/mL (C) of MT-II. The effect of preincubation of cells with 2 mM EGTA before the addition of the toxin was determined. Controls included cells incubated with medium alone without MT-II (C).

pain and inflammatory events (Lomonte and Gutiérrez, 1989; Lomonte et al., 1994a; Chacur et al., 2003; Zuliani et al., 2005). Our observations (Mora et al., 2005 and this work) show that this protein induces a spectrum of cellular responses, ranging from proliferative to necrotic outcomes, in a lymphoblastoid cell line in culture. Since Ca^{2+} plays a key role in a wide variety of physiologic and pathologic cellular events (Nicotera et al., 1990; Berridge et al., 2000, 2003; Orrenius et al., 2003), its role in MT-II-induced effects was assessed. The present results demonstrate dose- and time-dependent increments in cytosolic Ca^{2+} concentrations induced by MT-II. A parallel determination of

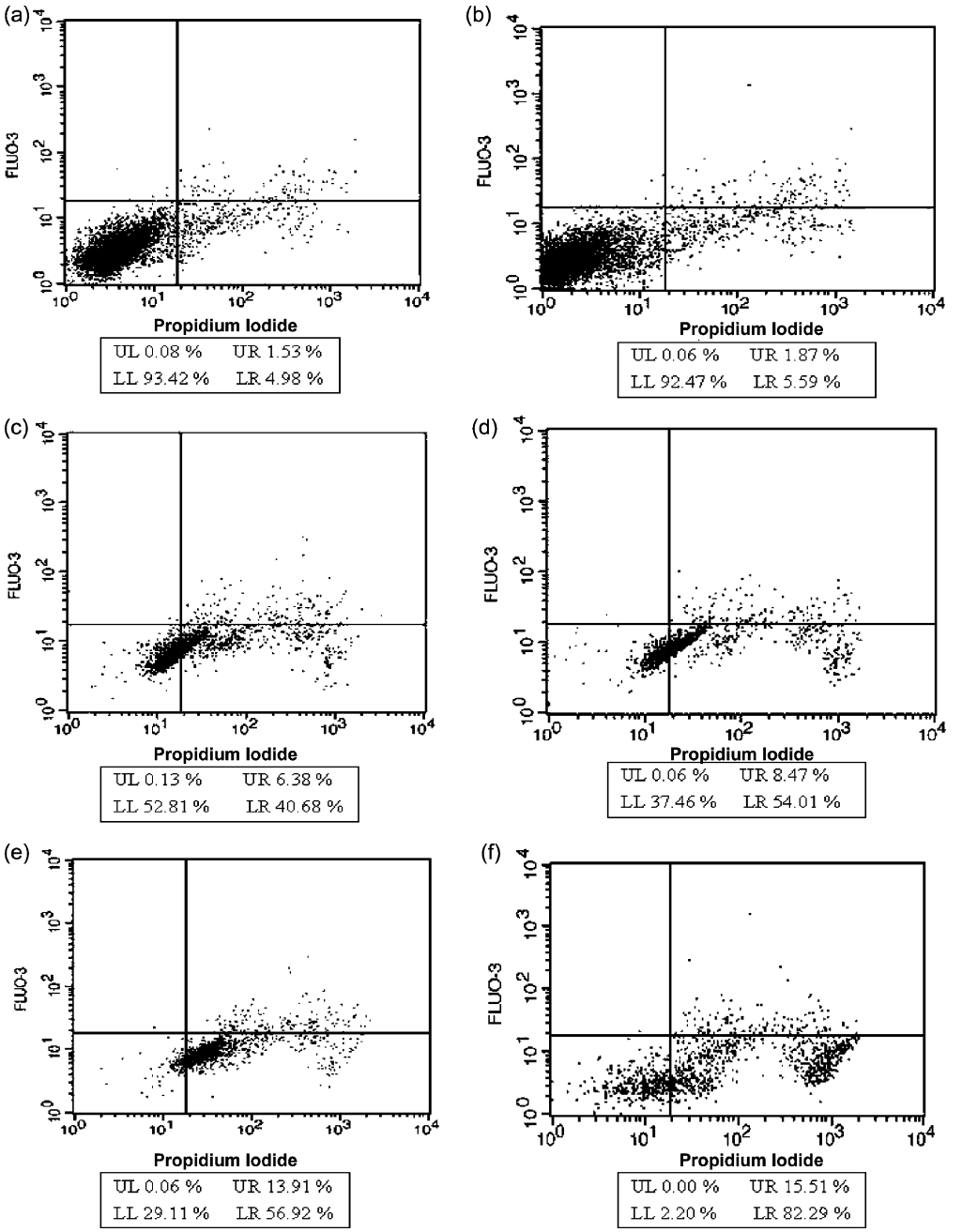

Fig. 3. Flow cytometric analysis of cytosolic Ca^{2+} concentration (Fluo-3 fluorescence) and plasma membrane disruption (penetration of PI), in lymphoblastoid cells incubated with MT-II. Cells were incubated for 20 min with medium alone without toxin (A) or with the following concentrations of MT-II: (B) 0.5 μg/mL, (C) 12.5 μg/mL, (D) 25 μg/mL, (E) 50 μg/mL, and (F) 100 μg/mL. A dose-dependent increment in cytosolic Ca^{2+} is associated with penetration of PI as a consequence of plasma membrane disruption.

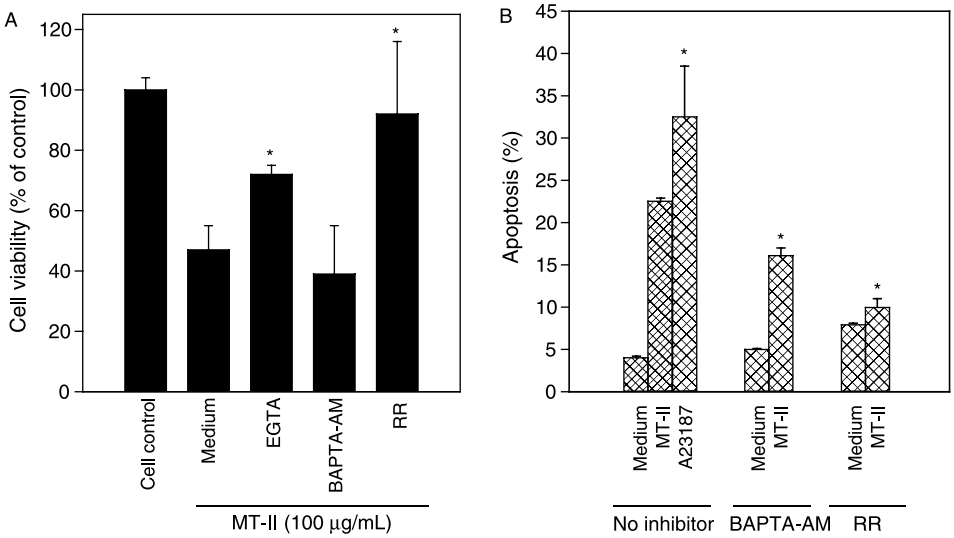

Fig. 4. Effect of EGTA, BAPTA-AM and ruthenium red (RR) on necrosis (A) and apoptosis (B) induced by MT-II in lymphoblastoid cells. Necrosis was assessed by the XTT reduction assay after 24 h of incubation with a toxin concentration of 100 μg/mL, and apoptosis was determined by the TUNEL assay after 48 h incubation with a toxin concentration of 12.5 μg/mL. Controls were incubated with medium without toxin. Cells were preincubated with the various inhibitors before the addition of MT-II. In the case of apoptosis, a positive control was included in which cells were incubated with 25 μM A23187. Results are presented as mean ± SD. $*P < 0.05$ when compared with the effect induced by MT-II alone in the absence of inhibitors.

cytosolic Ca^{2+} concentration and staining by PI strongly suggests that plasma membrane disruption is the main mechanism behind the increments in cytosolic Ca^{2+}. MT-II, and related venom cytotoxic PLA_2s, are known to rapidly disrupt the integrity of artificial and cellular membranes (Gutiérrez et al., 1984; Díaz et al., 1991; Rufini et al., 1992; Lomonte et al., 1994a; Soares et al., 2000; Ward et al., 2002). A C-terminal region in Lys49 PLA_2 homologues, comprising a combination of cationic and hydrophobic residues, is involved in cellular and liposomal membrane

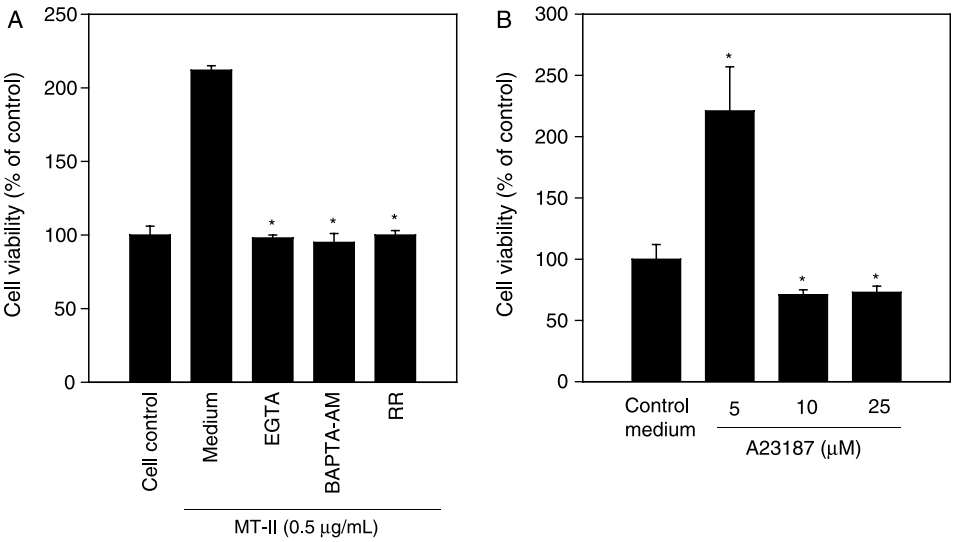

Fig. 5. (A) Effect of EGTA, BAPTA-AM and ruthenium red (RR) on cell proliferation induced by MT-II (0.5 μg/mL) in lymphoblastoid cells, assessed by the increment in the reduction of XTT after 24 h of incubation with the toxin. Control cells were incubated with medium alone. $*P < 0.05$ when compared with the effect induced by MT-II preincubated with medium instead of the inhibitors. (B) Effect of the ionophore A23187 in lymphoblastoid cell proliferation. Results are presented as mean ± SD. $*P < 0.05$ when compared with cell proliferation in cells incubated with medium alone (control medium).

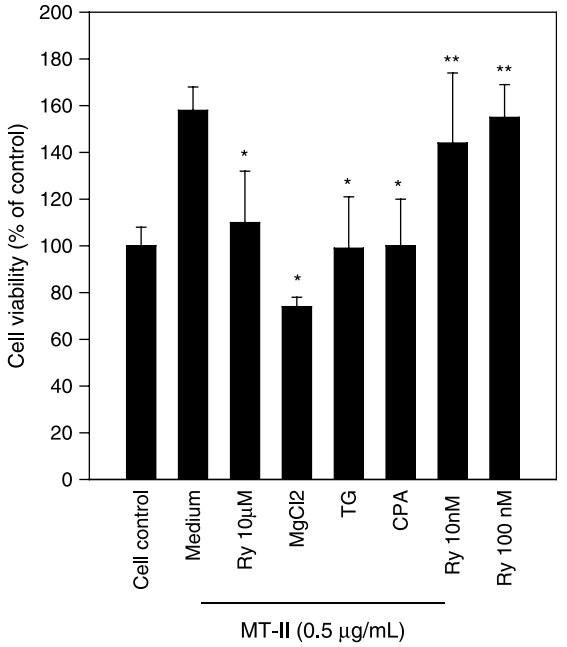

Fig. 6. Effect of ryanodine (Ry), $MgCl_2$, thapsigargin (TG) and cyclopiazonic acid (CPA) on cell proliferation induced by MT-II (0.5 μg/mL) in lymphoblastoid cells, assessed by the increment in the reduction of XTT after 24 h of incubation with the toxin. Control cells were incubated with medium alone. Lower concentrations of ryanodine (10 nM, 100 nM), in cells incubated without MT-II, promoted a proliferative effect similar to the one exerted by MT-II alone. Results are presented as mean ± SD. $*P < 0.05$ when compared with the effect induced by MT-II in cells that were preincubated with medium alone instead of the inhibitors. $**P < 0.05$ when compared with cells incubated with medium alone without MT-II (cell control).

disruption (Lomonte et al., 1994b, 2003; Chioato et al., 2002). Our findings suggest that the presence of a signal-transducing cellular receptor is not strictly required to exert these effects, which may be mediated solely by perturbation of the phospholipid bilayer.

At high toxin concentrations, necrosis was the predominant effect in lymphoblastoid cells, characterized by overt plasma membrane disruption, cellular and mitochondrial swelling, and nuclear pyknosis (Mora et al., 2005), alterations that have been described in muscle cells affected by *Bothrops* sp myotoxic PLA_2s (Gutiérrez et al., 1984, 1991). In these circumstances, a prominent and rapid Ca^{2+} influx occurs, following the steep electrochemical gradient normally maintained across the plasma membrane. Pronounced increments in cytosolic Ca^{2+} concentration are associated with the onset of cellular degenerative events, such as cytoskeletal and mitochondrial derrangements, activation of calpains and cytosolic PLA_2s, deregulation of metabolic pathways and ATP depletion (Nicotera et al., 1990; Gutiérrez and Ownby, 2003). Chelation of extracellular Ca^{2+} by EGTA significantly reduced cytotoxicity, thus supporting a significant role of Ca^{2+} influx in this pathologic event. This effect of EGTA is not due to a Ca^{2+} dependence of MT-II action, since this protein disrupts membranes in a Ca^{2+}-independent fashion (Díaz et al., 1991; Rufini et al., 1992). In contrast, preincubation of cells with the cytosolic Ca^{2+} chelator BAPTA-AM did not reduce cytotoxicity at high MT-II concentrations, probably due to the drastic elevations of cytosolic Ca^{2+} taking place in these circumstances, which overcome the buffering capacity of BAPTA-AM. Interestingly, preincubation of cells with ruthenium red, an inhibitor of the mitochondrial uniporter Ca^{2+} transport, abolished MT-II-mediated cytotoxicity. It is suggested that a pronounced Ca^{2+} influx through the damaged plasma membrane results in the uniporter-mediated accumulation of this cation in mitochondria. This, in turn, may dissipate the proton gradient and activate the permeability transition pore to a high conductance state, drastically impairing mitochondrial function and leading the cell to irreversible damage, i.e. necrosis, as has been demonstrated with the ionophore A23187 (Quian et al., 1999). It seems, therefore, that Ca^{2+} accumulation by mitochondria does not play a buffering, protective role in this model, but instead contributes to the cell injury process.

When tested at a concentration of 12.5 μg/mL for 48 h, MT-II predominantly induced apoptosis, as previously described (Mora et al., 2005). Therefore, the predominant type of cytotoxic response observed, i.e. apoptosis or necrosis, depends on the toxin concentration and, consequently, on the extent of plasma membrane injury. A number of cytotoxic agents have been reported to induce apoptosis and necrosis depending on the intensity of their deleterious effects on cells (Orrenius et al., 1992; Leist et al., 1997; Plymale et al., 1999). In agreement with this concept, dose-dependent differences in the early increments in cytosolic Ca^{2+} were detected by our fluorescence microscope system, since when cells were treated with 100 μg/mL of MT-II there was a steep increase in cytosolic Ca^{2+}, whereas a less pronounced increment occurred when using a MT-II concentration of 12.5 μg/mL. Thus, it is suggested that the apoptotic/necrotic dichotomy observed in our model may depend on different Ca^{2+} threshold points associated with these pathologic outcomes. In contrast with necrosis, MT-II-induced apoptosis was inhibited by the cytosolic Ca^{2+} chelator BAPTA-AM. It is likely that the lower increments in Ca^{2+} associated with apoptosis are readily controlled by BAPTA-AM, thus supporting the hypothesis that increase in cytosolic Ca^{2+} levels plays a key role in activating apoptotic pathways. In support of this, ionophore A23187 (25 μM) was also able to induce apoptosis in this model. Ca^{2+} exerts a number of proapoptotic effects, such as calpain-mediated caspase activation, activation of cytosolic PLA_2, generation of reactive oxygen species and nitric oxide, exposure of phosphatydylserine, activation of calcineurin and formation of the mitochondrial permeability transition pore (Orrenius et al., 2003).

As in the case of necrosis, ruthenium red also inhibited apoptosis, stressing the role of mitochondrial Ca^{2+} loading in the onset this effect, probably through the formation of the permeability transition pore at a subnecrotic level, with the consequent release of proapoptotic proteins from this organelle, such as cytochrome C and SMAC/DIABLO (Orrenius et al., 2003). Apoptosis in a similar cell line has been shown to be Ca^{2+}-dependent (Bonnefoy et al., 1994). In addition, the protective effect of ruthenium red in both apoptosis and necrosis may be related to the role of ATP in cell survival. Ca^{2+} sequestration by mitochondria may impair the machinery of ATP synthesis, thus reducing cellular ATP to levels incompatible with cell survival, leading cells to apoptotic or necrotic cell death, an outcome that depends on the extent of membrane lesion and Ca^{2+} influx. Despite the fact that inhibition of mitochondrial Ca^{2+} uniporter is the most common effect adscribed to ruthenium red, this compound may also affect the release of this cation from other intracellular sources (Griffiths, 2000). Therefore, the described effects of ruthenium red in our experiments may also depend on this alternative action, an issue that remains open for future studies.

Besides the toxic effects discussed above, MT-II induces a proliferative response in this cell line (Mora et al., 2005). Previously, Rufini et al. (1996) described a similar response in fibroblasts treated with low concentrations of a catalytically-inactive Ser49 PLA_2 from the venom of *Vipera ammodytes*. In our case a toxin concentration of 0.5 μg/mL, which was not cytotoxic but induced proliferation, increased cytosolic Ca^{2+} levels to approximately 5 μM. EGTA and BAPTA-AM inhibited the proliferative effect, thus implicating a role for a Ca^{2+} influx in this response. This agrees with experiments performed with a low concentration of A23187, in which a proliferative response was observed. Furthermore, the involvement of the CICR mechanism in this effect was evidenced by the finding that it was inhibited by the previous depletion of Ca^{2+} reserves of endoplasmic reticulum by thapsigargin and cyclopiazonic acid. Moreover, inhibition of the ryanodine channel also abrogated cellular proliferation. Taken together, these observations suggest that, at low concentrations, MT-II induces a perturbation of plasma membrane which results in a Ca^{2+} influx that causes a small increment in cytosolic Ca^{2+} levels. This, in turn, is likely to activate the mechanism of CICR, generating the oscillations in cytosolic Ca^{2+} observed in our experiments. It is suggested that Ca^{2+} oscillations associated with this effect are achieved through a concerted functional unit constituted by SERCA and the ryanodine receptor, with the possible participation of the inositol triphosphate (IP3) receptor.

In addition, the inhibitory effect of ruthenium red in proliferation strongly suggests that mitochondria are also involved, probably through the regulation of the Ca^{2+} signal amplitude (Schuster et al., 2002). Mitochondria form quasi-synapses with the endoplasmic reticulum, modulating the local Ca^{2+} concentrations in the vicinity of IP3 and ryanodine channels (Selivanov et al., 1998; Berridge et al., 2000, 2003). This fact underlines the possible role of the oscillatory behavior specificity, and the relevance of the modulation of this Ca^{2+} signal, by different elements of the Ca^{2+} toolkit, to codify for a determined response, in this case proliferation. The effectors of this signal remain unknown, but Ca^{2+}-dependent protein kinases are good candidates.

In conclusion, the various cellular responses to different doses of a Lys49 PLA_2 homologue are associated with changes in the permeability of the plasma membrane which, depending on their intensity, induce variable increments in cytosolic Ca^{2+} levels. Inhibition of this influx greatly reduces the extent of MT-II-induced necrosis, apoptosis and proliferation. In addition, blockade of the mitochondrial Ca^{2+} uniporter also inhibits these effects, thus implicating this organelle in the cellular degenerative events described. At cytotoxic MT-II concentrations, the predominant type of cellular degenerative response, i.e. apoptosis or necrosis, is likely to depend on the extent of cytosolic Ca^{2+} increment and the Ca^{2+} thresholds of these pathologic phenomena. Lower toxin concentrations induce a proliferative response associated with an oscillatory Ca^{2+} increment involving changes in plasma membrane permeability, endoplasmic reticulum reserves and mitochondria.

Acknowledgements

The authors thank Cecilia Díaz and Bruno Lomonte for fruitful discussions, and Javier Núñez, Francisco Vega, Federico Ruiz, Juan Carlos Villalobos and Rodrigo Chaves for their valuable collaboration in the laboratory. This work was supported by grants from Vicerrectoría de Investigación, Universidad de Costa Rica. This manuscript was presented in partial fulfillment of the requisites for the MSc degree of R. Mora at the University of Costa Rica.

References

Berridge, M.J., Lipp, P., Bootman, M.D., 2000. The versatility and universality of calcium signaling. Nat. Rev. Mol. Cell Biol. 1, 11–21.

Berridge, M.J., Bootman, M.D., Roderick, H.L., 2003. Calcium signalling: dynamics, homeostasis and remodelling. Nat. Rev. Mol. Cell Biol. 4, 517–529.

Bonnefoy, N., Genestier, L., Flacher, M., Revillard, J.P., 1994. The phosphoprotein phosphatase calcineurin controls calcium-dependent apoptosis in B cell lines. Eur. J. Immunol. 24, 325–329.

Brusés, J.L., Capaso, J., Katz, E., Pilar, G., 1993. Specific in vitro biological activity of snake venom myotoxins. J. Neurochem. 60, 1030–1042.

Bultrón, E., Thelestam, M., Gutiérrez, J.M., 1993. Effects on cultured mammalian cells of myotoxin III, a phospholipase A_2 isolated from *Bothrops asper* (terciopelo) venom. Biochim. Biophys. Acta 1179, 253–259.

Bunn, P.A., Dienhart, D.G., Chan, D., Puck, T.T., Tagawa, M., Jewett, P.B., Braunschweiger, E., 1990. Neuropeptide stimulation of calcium flux in human lung cancer cells: delineation of alternative pathways. Proc. Natl Acad. Sci. USA 87, 2162–2166.

Burchiel, S.W., Edwards, B.S., Kuckuck, F.W., Lauer, F.T., Prossnitz, E.R., Ransom, J.T., Sklar, L.A., 2000. Analysis of free intracellular calcium by flow cytometry: multiparameter and pharmacologic applications. Methods 21, 221–230.

Chacur, M., Longo, I., Picolo, G., Gutiérrez, J.M., Lomonte, B., Guerra, J.L., Teixeira, C.F.P., Cury, Y., 2003. Hyperalgesia induced by Asp49 and Lys49 phospholipases A_2 from *Bothrops asper* snake venom: pharmacological mediation and molecular determinants. Toxicon 41, 667–678.

Chioato, L., de Oliveira, A.H., Ruller, R., Sa, J.M., Ward, R.J., 2002. Distinct sites for myotoxic and membrane-damaging activities in the C-terminal region of a Lys49-phospholipase A_2. Biochem. J. 366, 971–976.

Cudd, L., Clarke, C., Clinkenbeard, K., 2003. Contribution of intracellular calcium stores to an increase in cytosolic calcium concentration induced by *Mannheimia haemolytica* leukotoxin. FEMS Micobiol Lett. 225, 23–27.

Dennis, E.A., 1994. Diversity of group types, regulation, and function of phospholipase A_2. J. Biol. Chem. 269, 13057–13060.

Díaz, C., Gutiérrez, J.M., Lomonte, B., Gené, J.A., 1991. The effect of myotoxins isolated from *Bothrops* snake venoms on multilamellar liposomes: relationship to phospholipase A_2, anticoagulant and myotoxic activities. Biochim. Biophys. Acta 1070, 455–460.

Goldbeter, A., 2002. Computational approaches to cellular rhythms. Nature 420, 238–245.

Griffiths, E.J., 2000. Use of ruthenium red as an inhibitor of mitochondrial Ca^{2+} uptake in single rat cardiomyocytes. FEBS Lett. 486, 257–260.

Gutiérrez, J.M., Lomonte, B., 1989. Local tissue damage induced by *Bothrops* snake venoms. A review. Mem. Inst. Butantan 51, 211–223.

Gutiérrez, J.M., Lomonte, B., 2003. Efectos locales en el envenenamiento ofídico en América Latina. In: Cardoso, J.L.C., Franca, F.O.S., Hui, F.W., Málaque, C.M.S., Haddad, V. (Eds.), Animais Peconhentos no BrasilBiologia, Clínica e Terapeutica dos Accidentes. Sarvier, Sao Paulo, pp. 310–323.

Gutiérrez, J.M., Lomonte, B., Chaves, F., Moreno, E., Cerdas, L., 1986. Pharmacological activities of a toxic phospholipase A isolated from the venom of the snake *Bothrops asper*. Comp. Biochem. Physiol. 84C, 159–164.

Gutiérrez, J.M., Núñez, J., Díaz, C., Cintra, A.C.O., Homsi-Brandeburgo, M.I., Giglio, J.R., 1991. Skeletal muscle degeneration and regeneration after injection of bothropstoxin-II, a phospholipase A_2 isolated from the venom of the snake *Bothrops jararacussu*. Exp. Mol. Pathol. 55, 217–229.

Gutiérrez, J.M., Ownby, C.L., 2003. Skeletal muscle degeneration induced by venom phospholipases A_2: insights into the mechanisms of local and systemic myotoxicity. Toxicon 42, 915–931.

Gutiérrez, J.M., Ownby, C.L., Odell, G.V., 1984. Pathogenesis of myonecrosis induced by crude venom and a myotoxin of *Bothrops asper*. Exp. Mol. Pathol. 40, 367–379.

Harris, J.B., Cullen, M.J., 1990. Muscle necrosis caused by snake venoms and toxins. Electron Microsc. Rev. 3, 183–211.

Johnson, J.D., Klausen, C., Habibi, H.R., Chang, J.P., 2002. Function-specific calcium stores selectively regulate growth hormone secretion, storage, and mRNA level. Am. J. Physiol. Endocrinol. Metab. 282, E810–E819.

Kini, R.M., 1997. Phospholipase A_2—a complex multifunctional protein puzzle. In: Kini, R.M. (Ed.), Venom Phospholipase A_2 Enzymes: Structure, Function and Mechanism. Wiley, Chichester, p. 1.

Kini, R.M., Chan, Y.M., 1999. Accelerated evolution and molecular surface of venom phospholipase A_2 enzymes. J. Mol. Evol. 48, 125–132.

Laemmli, U.K., 1970. Cleavage of structural proteins during the assembly of the head of bacteriophage T4. Nature 227, 680–685.

Leist, M., Single, B., Cstoldi, A.F., Kuhnle, S., Nicotera, P., 1997. Intracellular adenosine triphosphate (ATP) concentration: a switch in the decision between apoptois and necrosis. J. Exp. Med. 185, 1481–1486.

Li, X., Traganos, F., Melamed, M.R., Darzynkiewicz, Z., 1995. Single step procedure for labeling DNA strand breaks with fluorescein- or BODIPY-conjugated deoxynucleotides. Detection of apoptosis and bromodeoxyuridine incorporation. Cytometry 20, 172–180.

Lomonte, B., Gutiérrez, J.M., 1989. A new muscle damaging toxin, myotoxin II, from the venom of the snake *Bothrops asper* (terciopelo). Toxicon 27, 725–733.

Lomonte, B., Tarkowski, A., Hanson, L.A., 1994a. Broad cytolytic specificity of myotoxin II, a lysine-49 phospholipase A_2 of *Bothrops asper* snake venom. Toxicon 32, 1359–1369.

Lomonte, B., Moreno, E., Tarkowski, A., Hanson, L.A., Maccarana, M., 1994b. Neutralizing interaction between heparins and myotoxin II, a Lysine 49 phospholipase A_2 from *Bothrops asper* snake venom. Identification of a heparin-binding and cytolytic toxin region by the use of synthetic peptides and molecular modeling. J. Biol. Chem. 269, 29867–29873.

Lomonte, B., Angulo, Y., Calderón, L., 2003. An overview of lysine-49 phospholipase A_2 myotoxins from crotalid snake venoms and their structural determinants of myotoxic action. Toxicon 42, 885–901.

Mora, R., Valverde, B., Díaz, C., Lomonte, B., Gutiérrez, J.M., 2005. A Lys49 phospholipase A_2 homologue from *Bothrops asper* snake venom induces proliferation, apoptosis and necrosis in a lymphoblastoid cell line. Toxicon 45, 651–660.

Nicotera, P.L., Bellomo, G., Orrenius, S., 1990. The role of Ca^{2+} in cell killing. Chem. Res. Toxicol. 3, 484–494.

Novak, E.J., Rabinovitch, P.S., 1994. Improved sensitivity in flow cytometric intracellular ionized calcium measurement using Fluo-3/Fura Red fluorescence ratios. Cytometry 17, 135–141.

Ohno, M., Ogawa, T., Oda-Ueda, N., Chijiwa, T., Hattori, S., 2002. Accelerated and regional evolution of snake venom gland isozymes. In: Ménez, A. (Ed.), Perspectives in Molecular Toxinology. Wiley, New York, pp. 387–400.

Ohno, M., Chijiwa, T., Oda-Ueda, N., Ogawa, T., Hattori, S., 2003. Molecular evolution of myotoxic phospholipases A_2 from snake venom. Toxicon 42, 841–854.

Orrenius, S., Burkitt, M., Kass, G., Dypbukt, J., Nicotera, P., 1992. Calcium ions and oxidative cell injury. Ann. Neurol. 32, S33–S42.

Orrenius, S., Zhivotovsky, B., Nicotera, P., 2003. Regulation of cell death: the calcium-apoptosis link. Nature Rev. Mol. Cell Biol. 4, 552–565.

Ownby, C.L., Selistre de Araujo, H.S., White, S.P., Fletcher, J.E., 1999. Lysine 49 phospholipase A_2 proteins. Toxicon 37, 411–445.

Páramo, L., Lomonte, B., Pizarro-Cerdá, J., Bengoechea, J.A., Gorvel, J.P., Moreno, E., 1998. Bactericidal activity of Lys49 and Asp49 myotoxic phospholipases A_2 from *Bothrops asper* snake venom. Synthetic Lys49 myotoxin II-(115–129)-peptide identifies its bactericidal region. Eur. J. Biochem. 253, 452–461.

Plymale, D., Comerdelle, A., Fermin, C., Martin, D., Costin, J., Norris, C., Burroughs, S., Mietzer, T., Montelaro, R., Garry, R., 1999. Concentration-dependent differential induction of necrosis or apoptosis by HIV-1 lytic peptide 1. Peptides 20, 1275–1283.

Quian, T., Herman, B., Lemasters, J., 1999. The mitochondrial permeability transition mediates both necrotic and apoptotic death of hepatocytes exposed to Br-A23187. Toxicol. Appl. Pharmacol. 154, 117–125.

Rigual, R., Montero, M., Rico, A.J., Prieto-Lloret, J., Alonso, M.T., Alvarez, J., 2002. Modulation of secretion by the endoplasmic reticulum in mouse chromaffin cells. Eur. J. Neurosci. 16, 1690–1696.

Rosenberg, P., 1990. Phospholipases. In: Shier, W.T., Mebs, D. (Eds.), Handbook of Toxinology. Marcel Dekker, New York, pp. 67–277.

Rufini, S., Cesaroni, P., Desideri, A., Farias, R., Gubensek, F., Gutiérrez, J.M., Luly, P., Massoud, R., Morero, R., Pedersen, J.Z., 1992. Calcium ion independent membrane leakage induced by phospholipase-like myotoxins. Biochemistry 31, 12424–12430.

Rufini, S., Cesaroni, M.P., Balestro, N., Luly, P., 1996. Proliferative effect of ammodytin L from the venom of *Vipera ammodytes* on 208F rat fibroblasts in culture. Biochem. J. 320, 467–472.

Scheenen, W.J., Makings, L.R., Gross, L.R., Pozzan, T., Tsien, R.Y., 1996. Photodegradation of Indo-1 and its effect on apparent Ca^{2+} concentrations. Chem. Biol. 3, 765–774.

Schuster, S., Marhl, M., Hofer, T., 2002. Modelling of simple and complex calcium oscillations. From single-cell responses to intercellular signalling. Eur. J. Biochem. 269, 1333–1355.

Selivanov, V.A., Ichas, F., Holmuhamedov, E.L., Jouaville, L.S., Evtodienko, Y.V., Mazat, J.P., 1998. A model of mitochondrial Ca^{2+}-induced Ca^{2+} release simulating the Ca^{2+} oscillations and spikes generated by mitochondria. Biophys. Chem. 72, 111–121.

Shakhman, O., Herkert, M., Rose, C., Humeny, A., Becker, C.M., 2003. Induction by β-bungarotoxin of apoptosis in cultured hippocampal neurons is mediated by Ca^{2+}-dependent formation of reactive oxygen species. J. Neurochem. 87, 598–608.

Six, D.A., Dennis, E.A., 2000. The expanding superfamily of phospholipase A_2 enzymes: classification and characterization. Biochim. Biophys. Acta 1488, 1–19.

Soares, A.M., Andriao-Escarso, S.H., Angulo, Y., Lomonte, B., Gutiérrez, J.M., Toyama, M.H., Marangoni, S., Arni, R.K., Giglio, J.R., 2000. Structural and functional characterization of myotoxin I, a Lys49 phospholipase A_2 homologue from *Bothrops moojeni* (caissaca) snake venom. Arch. Biochem. Biophys. 373, 7–15.

Su, S.H., Su, S.J., Lin, S., Chang, K.L., 2003. Cardiotoxin III selectively enhances activation-induced apoptosis of human CD8 + T lymphocytes. Toxicol. Appl. Pharmacol. 193, 97–105.

Teixeira, C.F.P., Landucci, E.C.T., Antunes, E., Chacur, M., Cury, Y., 2003. Inflammatory effects of snake venom myotoxic phospholipases A_2. Toxicon 42, 947–962.

Valentin, E., Lambeau, G., 2000. What can venom phospholipases A_2 tell us about the functional diversity of mammalian secreted phospholipases A_2? Biochimie 82, 815–831.

van den Bergh, C.J., Slotboom, A.J., Verheij, H.M., de Haas, G.H., 1988. The role of aspartic acid-49 in the active site of phospholipase A_2. A site-specific mutagenesis study of porcine pancreatic phospholipase A_2 and the rationale of the enzymatic activity of [lysine49] phospholipase A_2 from *Agkistrodon piscivorus piscivorus*' venom. Eur. J. Biochem. 176, 353–357.

Vázquez-Martínez, O., Cañedo-Merino, R., Díaz-Muñoz, M., Riesgo-Escovar, J.R., 2003. Biochemical characterization, distribution and phylogenetic analysis of *Drosophila melanogaster* ryanodine and IP3 receptors, and thapsigargin-sensitive Ca^{2+}-ATPase. J. Cell Sci. 116, 2483–2494.

Ward, R.J., Chioato, L., de Oliveira, A.H.C., Ruller, R., Sá, J.M., 2002. Active-site mutagenesis of a Lys49-phospholipase A_2: biological and membrane-disrupting activities in the absence of catalysis. Biochem. J. 362, 89–96.

Williams, D., Fay, F., 1990. Intracellular calibration of the fluorescent calcium indicator Fura-2. Cell Calcium 11, 75–83.

Zuliani, J.P., Fernandes, C.M., Zamuner, S.R., Gutiérrez, J.M., Teixeira, C.F.P., 2005. Inflammatory events induced by Lys-49 and Asp-49 phospholipases A_2 isolated from *Bothrops asper* snake venom: role of catalytic activity. Toxicon 45, 335–346.